Proton Inelastic Scattering from the Five Stable, Even-Mass Isotopes of Molybdenum*

H. F. Lutz, D. W. Heikkinen, and W. Bartolini
Lawrence Radiation Laboratory, University of California, Livermore, California 94550
(Received 9 April 1971)

Elastic and inelastic scattering of 15-MeV protons, accelerated by the 90-in. cyclotron at Lawrence Radiation Laboratory, Livermore, from isotopically enriched targets of ^{92,94,96,98,100}Mo were studied with an over-all resolution of 50 keV (full width at half maximum). The experimental angular distributions were analyzed using a coupled-channel calculation. The collective vibrational model was employed to describe the states of the nucleus. Fifty angular distributions of scattered particles were measured and all but three were fitted with theoretical curves. The results for ^{92}Mo, which has a closed neutron shell associated with the magic number $N = 50$, are discussed separately. All the inelastic scattering to levels in ^{92}Mo were fitted with single-step processes. The other even-mass isotopes of molybdenum were analyzed first by considering the main quadrupole and octupole vibrational states and then considering the states that can be described as possible mixtures of one- and two-quadrupole phonons. A high degree of single-phonon admixture was found to be present. Finally the weaker states were considered with the simple 0^+-I^π coupling scheme. Electromagnetic transition rates were inferred from the deformabilities deduced in the present experiment. The results are compared with other experiments.

I. INTRODUCTION

The even-mass isotopes of molybdenum that we study with inelastic proton scattering range from the nucleus ^{92}Mo, which can be adequately described by the spherical shell model with a few active orbits, to ^{100}Mo, which has an appreciable quadrupole moment and has not been described successfully with the shell model. As an example of the difference between these isotopes, the present experiment shows that the integrated cross section for exciting the first quadrupole state is only 7.2 mb in ^{92}Mo and a sizable 40.0 mb in ^{100}Mo.

This paper is the fourth in a series of proton scattering studies that make use of a nuclear vibrational model[1,2] to describe the excited states of the nuclei and employ the coupled-channel calculation[3] in the form of Tamura's[4,5] computer code to analyze the experimental data. We have reported previously similar experiments on the even-mass isotopes of cadmium,[6] titanium,[7] and germanium.[8]

The coupled-channel calculation can treat both single-step and multiple-step processes. This is especially important for considering the excitation of levels whose description may be in terms of two or more phonons. The computer code that we use includes spin-orbit distortion, complex form factor, and Coulomb excitation. The strength parameters that enter the calculation can be varied and need not be those assigned by the vibrational model. It is also possible to describe states as mixtures of one- and two-phonon states.

A number of shell-model calculations have been performed[9-15] in the $A = 90$ region. The shell-model description of ^{92}Mo assumes an inert core of ^{88}Sr with the valence protons filling the $2p_{1/2}$ and $1g_{9/2}$ single-particle orbitals.[15] Lanford[16] has shown that seniority is good for identical nucleons in $j = \frac{9}{2}$ orbitals. He has derived a residual interaction that correctly interprets the 2^+, 4^+, 6^+, 8^+ spectrum seen in ^{92}Mo. Beyond $N = 50$ the neutrons that appear in the calculation when the heavier isotopes of molybdenum are considered enter the $2d_{5/2}$ shell. Vervier[13] has made shell-model calculations for the energy levels of molybdenum with neutron number N between 50 and 56. The heaviest isotope of molybdenum that we consider, ^{100}Mo, has 8 neutrons outside the closed shell at $N = 50$.

Previous work on inelastic scattering has emphasized ^{92}Mo. Dickens *et al.*[17] investigated the level structure with 10-MeV protons and Martens and Bernstein[18] studied it with 31-MeV α-particle scattering. The levels of ^{92}Mo were studied by in-beam γ-ray spectroscopy performed by Jaklevic, Lederer, and Hollander[19] and Lieb, Hausmann, and Kent[20] have studied the ^{92}Mo$(p, p'\gamma)$ reaction via isobaric analog resonances.

Information on the other isotopes of molybdenum has come mainly from decay experiments. The nucleus ^{94}Mo has been studied with the $(^3\text{He}, d)$ reaction by Cates, Ball, and Newman[21] and the decay of ^{94}Tc by Aras, Eichler, and Chilosi[22] and Barrette, Boutard, and Munaro.[23] For ^{96}Mo Eichler[24] has studied the circular polarization of γ rays after the capture of thermal neutrons, and Antman *et al.*[25] have performed an internal-conversion study. The reaction ^{98}Mo$(p, p'e)$ via isobaric resonances has been studied by Courtney and Moore.[26] Infor-

TABLE I. Isotopic compositions of Mo targets used in the present experiment.

at.%	Target ^{92}Mo	^{94}Mo	^{96}Mo	^{98}Mo	^{100}Mo
92	97.6	0.87	0.18	0.31	0.60
94	0.73	93.9	0.18	0.23	0.23
95	0.46	2.85	0.94	0.49	0.40
96	0.33	1.04	96.8	0.61	0.81
97	0.16	0.40	0.96	0.77	0.36
98	0.48	0.75	0.82	97.0	1.69
100	0.23	0.22	0.10	0.59	95.9

mation about the levels of ^{98}Mo has also been obtained by Evans and Ajzenberg-Selove[27] using the ^{97}Mo$(d, p)^{98}$Mo reaction and by Hubenthal, Monnand, and Moussa[28] who studied the radioactive decay of ^{98}Nb isomers.

The work of the University of Kentucky groups[29,30] who studied the Mo$(n, n'\gamma)$ reactions for the stable, even-mass isotopes of molybdenum with low-energy neutrons has been very helpful for the present work. Where possible we have used their energy level assignments, made with Ge(Li) detectors, to label the groups we see in the proton inelastic scattering at 15 MeV.

II. EXPERIMENTAL METHOD

The experimental techniques used in the present experiment were similar to those described previously in this series.[6-8] Protons were accelerated to 15 MeV by the Livermore variable energy cyclotron. The beam was momentum-analyzed by a 90° bending magnet with a 76.2-cm radius of curvature and focused to a spot at the center of a 60.9-cm-diam scattering chamber. The beam was monitored by a Faraday-cup and current digitizer.

The isotopic composition of each of the self-supporting targets, which were supplied by the isotopes division of Oak Ridge National Laboratory is given in Table I. Each of the targets had an areal density of approximately 500 μg cm^{-2} but were extremely nonuniform. We found it necessary to normalize the cross sections to the forward angle elastic scattering predictions made with the optical-model parameters listed in Table II.

TABLE II. Optical-model parameters and deformation parameters for first quadrupole and octupole states. Parameters common to all isotopes: $r_0 = 1.25$ fm, $r_c = 1.25$ fm, $W = 0.0$ MeV, $a = 0.65$ fm, $V_{so} = 5.0$ MeV, $\bar{a} = 0.47$ fm.

Isotope	V (MeV)	W_D (MeV)	E_x (keV)	I^π	β_{0I}	β_{0I} (EM) (Ref. 33)
^{92}Mo	51.5	13.4	1510	2^+	0.105	0.116
			2850	3^-	0.174	
^{94}Mo	52.0	13.8	871	2^+	0.160	0.169
			2533	3^-	0.163	
^{96}Mo	52.5	14.3	777	2^+	0.175	0.175
			2230	3^-	0.185	
^{98}Mo	52.9	14.6	788	2^+	0.168	0.168
			2024	3^-	0.195	
^{100}Mo	53.4	15.0	534	2^+	0.226	0.253
			1910	3^-	0.210	

A single lithium-drifted silicon detector 2000 μm thick, operated at 300-V reverse bias and subtending 2.5×10^{-4} sr, was used to observe the scattered protons. Thermoelectric coolers were used to cool the detectors to −25°C to minimize leakage currents. The over-all resolution of the present experiment was 50 keV (full width at half maximum).

III. EXPERIMENTAL RESULTS AND COUPLED-CHANNEL ANALYSIS

A. Experimental Results

As previously noted, because the targets were nonuniform we found it necessary to normalize the results to the forward angle elastic scattering prediction given by the optical model. The strengths

TABLE III. Energies, spins, parities, and integrated cross sections of levels seen in this work.

^{92}Mo			^{94}Mo			^{96}Mo			^{98}Mo			^{100}Mo		
E_X (keV)	I^π	σ_t (mb)	E_X (keV)	I^π	σ_t (mb)	E_X (keV)	I^π	σ_t (mb)	E_X (keV)	I^π	σ_t (mb)	E_X (keV)	I^π	σ_t (mb)
g.s.	0^+		g.s.	0^+		g.s.	0^+		g.s.	0^+		g.s.	0^+	
1510	2^+	7.2	871	2^+	17.9	777	2^+	23.6	736	0^+	1.2	534	2^+	40.0
2283	4^+	3.1	1573	4^+	4.9	1147	(0^+)	0.7	788	2^+	20.8	694	(0^+)	1.9
2527	5^-	3.1	1864	2^+	1.8	1495	2^+	2.3	1433	2^+	2.3	800	(2^+)	0.9
2613	6^+	1.2	2066	(0^+)	1.9	1624	4^+	3.1	1510	4^+	1.9	1063	2^+	4.7
2850	3^-	11.1	2421	(2^+)	1.8	1865	4^+	3.6	1760	2^+	0.8	1140	(4^+)	2.3
3110	(2^+)	3.1	2533	3^-	9.9	2230	3^-	11.9	2024	3^-	13.3	1463	(2^+)	0.8
			2580	(5^-)	1.8	2616	(4^+)	1.1	2208	(4^+)	2.1	1500	?	0.5
			2830	(4^+)	1.8	2732	(6^+)	1.3	2343	?	3.2	1768	?	0.5
			2930	(2^+)	1.6	2810	?	1.5	2450	(4^+)	1.1	1910	3^-	16.0
			3090	(2^+)	1.9	2990	(4^+)	2.0	2500	(3^-)	2.0			

of the real and imaginary parts of the optical-model potential shown in Table II were determined from the equations

$$V = 45.5 + 27.5\left[\frac{N-Z}{A}\right] + 0.4\frac{Z}{A^{1/3}},$$

$$W = 11.5 + 22\left[\frac{N-Z}{A}\right].$$

These are the same equations that gave adequate agreement for the cadmium isotopic sequence that we studied[8] previously. The dependence on neutron excess is in reasonable agreement with the results of Satchler[31] and Kossanyi-Demay and de Swiniarski.[32]

The levels seen in the present experiment are listed in Table III. This table contains the energies, spins, parities, and integrated cross sections. The integrated cross sections were obtained by fitting the experimental data with a sum of Legendre polynomials.

Figure 1 shows the position of the first quadrupole and octupole states in the even-mass isotopes of molybdenum. The length of the line that denotes the excitation energy is proportional to the enhancement of the transition over its single-particle estimate. This figure illustrates how the molybdenum isotopes become more collective as the neutron excess increases. The decrease in excitation energy and increase in deformability is more abrupt for the quadrupole states than it is for the octupole states. The experimental data and theoretical fits for the levels of each of the isotopes are displayed in Figs. 2–6. The errors displayed in the figures are statistical. All the cross sections in any one isotope have, of course, been normalized by the same factor determined by the forward angle elastic scattering. The theoretical fits to the data were determined by varying the values of the deformabilities and visually inspecting the results. The calculated cross sections are roughly proportional to the squares of the deformabilities or the $\beta(EL)$ one would deduce from these values. In our previous work[6] we estimated that the uncertainties in the $\beta(EL)$, due mainly to ambiguities in the combination of β and W_D, are about 15% for single-phonon and 30% for the two-phonon calculations.

B. Analysis of Results for ^{92}Mo

Since ^{92}Mo is such a good example of a spherical nucleus the coupling schemes used to analyze the data did not include the two-phonon type of calculation. Indeed, the analysis is equivalent to the ordinary distorted-wave-Born approximation (DWBA). It is more convenient to discuss the results for ^{92}Mo separately than to try to include it in the discussions of the other isotopes. The experimental angular distributions and theoretical fits are gathered in Fig. 2. The quality of the fits to the data is quite good. In Table IV we summarize the information obtained from these fits. It should be noted that the 2527-keV level has a

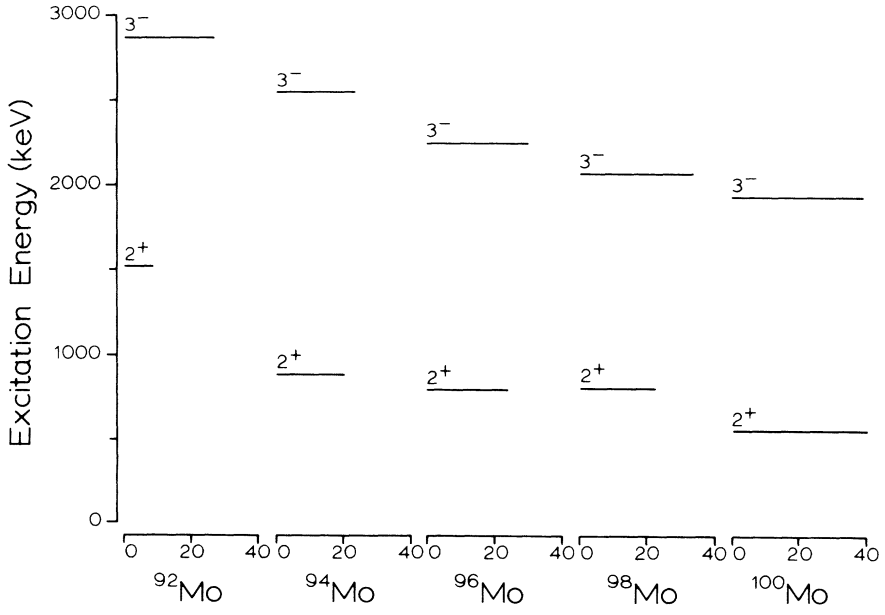

FIG. 1. The positions of the first quadrupole and octupole states in each isotope studied in the present experiment. The length of each line that indicates the energy of excitation is proportional to the value of $B(EL)$ expressed in single particle units. For ^{92}Mo $G(2)$ is 8.6 while for ^{100}Mo $G(2)$ is 40.1.

TABLE IV. Deformation parameters for ^{92}Mo deduced in the present experiment and comparison with the α-particle scattering results of Martens and Bernstein.[18]

E_X (keV)	I^π	β (present)	β (α)	$\beta \times (1.62/1.25)$ (α)
1510	2^+	0.105	0.080	0.104
2283	4^+	0.066	0.041	0.053
2527	5^-	0.05	0.053	0.069
2613	6^+	0.07	Not resolved	
2850	3^-	0.174	0.115	0.149
3110	(2^+)	0.07	0.044	0.057

neighbor at 2519 keV that we do not resolve. The fit to the known 5^- level was sufficiently good that we have assumed the other level to be only weakly excited. Vervier[13] predicts an excited 0^+ state between the known 4^+ and 5^- levels. If this is the 2519-keV state we would expect it to be very weakly excited in the present experiment. It could, however, be excited rather strongly in the low-energy experiments of the University of Kentucky group[29,30] where compound-nucleus processes should dominate.

Several calculations for two-step processes were performed. The 4^+ level at 2283 keV was assumed to be a two-quadrupole-phonon state and the 5^- level at 2527 keV a quadrupole-octupole-two-phonon state. The calculated cross sections were too low by 2 orders of magnitude. The $0^+ \rightarrow 5^-$ excitation should be interpreted as a $2p_{1/2}$ to $1g_{9/2}$ proton excitation. A calculation for a 0^+ excited state interpreted as a two-quadrupole-phonon state occurring at 2500 keV gave a maximum

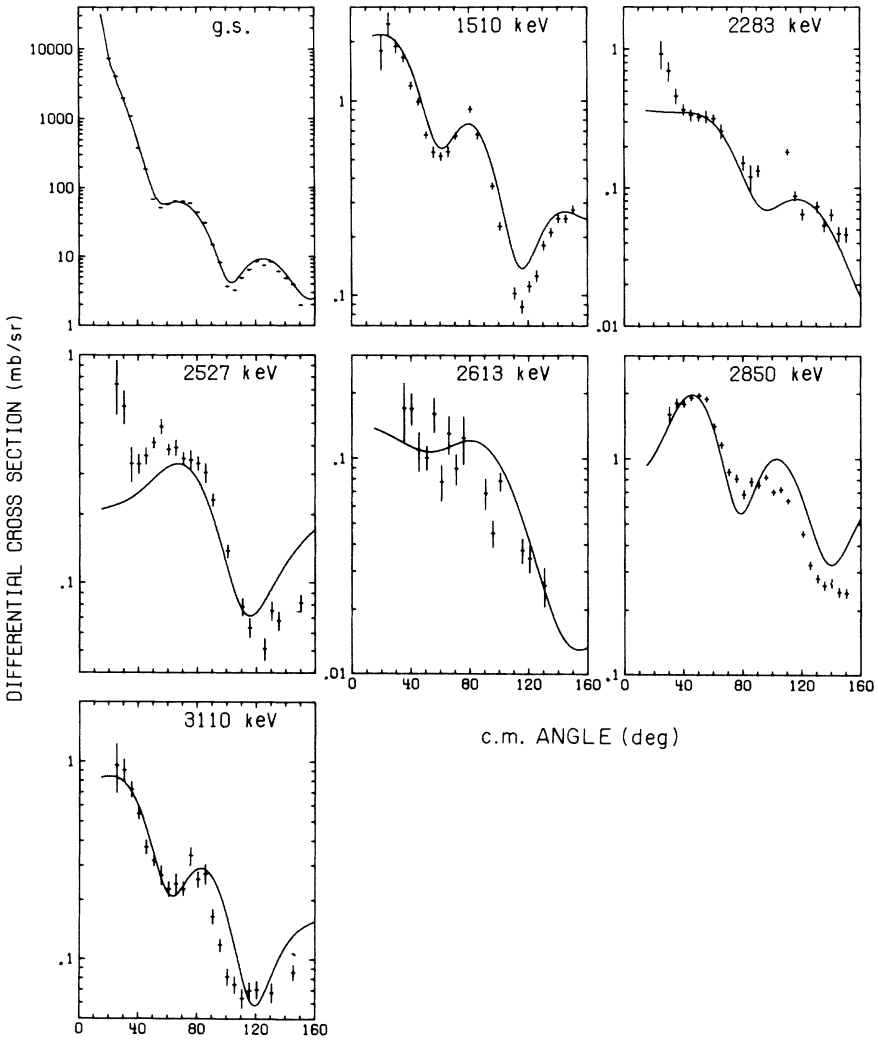

FIG. 2. Experimental angular distribution and theoretical fits for the inelastic scattering of 15-MeV protons from ^{92}Mo. Shown in this figure are examples of the quality of fits to a 2^+ (1510-keV), 3^- (2850-keV), 4^+ (2283-keV), 5^- (2527-keV), and 6^+ (2613-keV) level.

cross section of 15 μb sr^{-1} at 35°, which is too small to be seen in the present experiment.

In the same region of excitation energy Jaklevic, Lederer, and Hollander[19] observe a level that we do not see and, conversely, we see a level that they do not. The apparent discrepancies are, however, entirely understandable when one considers the selectivity of the reactions used in each experiment. Jaklevic, Lederer, and Hollander[19] studied the γ rays following the reaction ^{90}Zr(α, $2n$)-^{92}Mo. They see a level with $I^{\pi}=8^{+}$ at 2761 keV, which we do not see because of limitations on angular momentum transfer associated with the projectile and the direct excitation mechanism. On the other hand, we see an $I^{\pi}=3^{-}$ level at 2850 keV that they do not see. The negative-parity states in their experiment start with an 11^{-} level at 4487-keV excitation energy and are populated by successive $E2$ de-excitations. In ^{92}Mo the 3^{-} level occurs between the 7^{-} and 5^{-}, so the γ-ray cascade proceeds from the 5^{-} level at 2527 keV to the 4^{+} level at 2283 keV by an $E1$ transition.

For purposes of comparison we have included in Table IV some of the results of Martens and Bernstein[18] who employed 31-MeV α particles to study ^{92}Mo. When the different optical-model radii are taken into account the two experiments agree to within 20% except for the 5^{-} level at 2527 keV, which the α-particle experiment did not resolve from the 6^{+} level at 2613 keV. Neither experiment excited the 8^{+} level at 2761 keV. This indicates that the limitations on angular momentum transfer

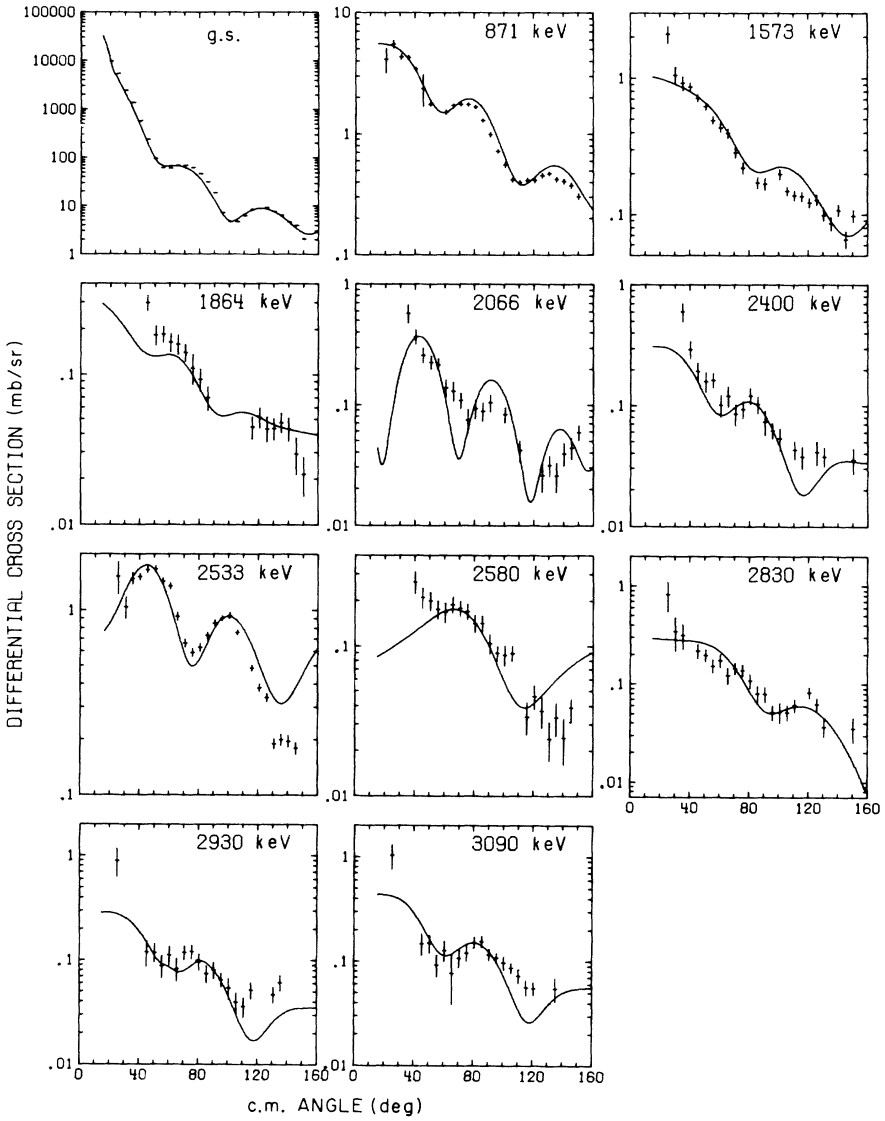

FIG. 3. Experimental results and theoretical fits for scattering to levels in ^{94}Mo.

is contained in the direct scattering mechanism and not necessarily in the momentum of the projectile.

In Fig. 2 we see examples of fits to states with $I^{\pi}=2^{+}$, 3^{-}, 4^{+}, 5^{-}, 6^{+}. The spins and parities are all well known. The quality is such that we can apply the analysis to the other isotopes and extract information with some degree of confidence.

C. Results for 0_0^+-2_1^+-3_1^- Coupling Scheme Applied to ^{94}Mo, ^{96}Mo, ^{98}Mo, and ^{100}Mo

The cross sections for exciting the first quadrupole and octupole states of each isotope were calculated using a 0_0^+-2_1^+-3_1^- coupling scheme where the subscripts indicate the number of vibrational phonons. The deformabilities deduced for these states are listed in Table II, which also contains for purposes of comparison the deformability determined by electromagnetic means and listed in the compilation of Stelson and Grodzins.[33] The values for the quadrupole deformabilities agree to within 10% except for the case of ^{100}Mo where the deviation is about 12%. The good quality of the theoretical fits to the elastic scattering and inelastic scattering to the first quadrupole and octupole states together with the reasonable agreement with the quadrupole deformation parameters determined by electromagnetic means indicates that our set of optical-model parameters and the nor-

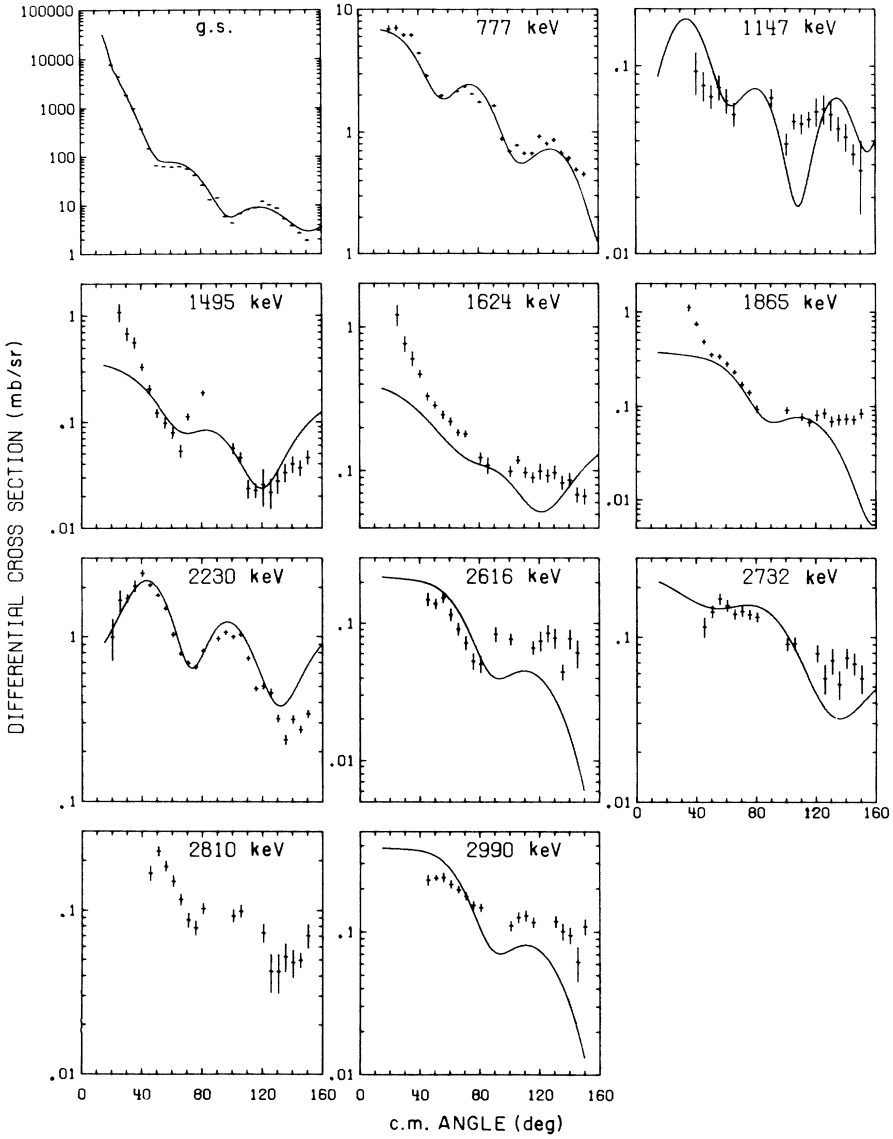

FIG. 4. Experimental results and theoretical fits for ^{96}Mo. No satisfactory fit was obtained for the scattering to the level at 2810 keV.

malization procedure for the experimental data are valid.

D. Results for 0_0^+-2_1^+-$0_{1,2}^+$-$2_{1,2}^+$ $4_{1,2}^+$ Coupling Scheme Applied to ^{94}Mo, ^{96}Mo, ^{98}Mo, and ^{100}Mo

In each of the isotopes studied with the exception of ^{92}Mo, there are states with $I^\pi = 0^+$, 2^+, 4^+ that we have analyzed within the 0_0^+-2_1^+-$0_{1,2}^+$-$2_{1,2}^+$-$4_{1,2}^+$ coupling scheme where, again, the subscripts indicate the number of phonons and the subscript 1, 2 indicates a mixture of one- and two-phonon states. This coupling scheme provides us with a framework for analysis and is not meant to imply that we are treating a two-quadrupole-phonon triplet in the sense of the collective vibrational model. The second 2^+ and first 4^+ states in these isotopes have an excitation energy about double the excitation energy of the first quadrupole state as one expects from the collective vibrational model. The position of the 0^+ excited state is not well behaved. In fact for ^{98}Mo it actually falls below the first quadrupole state at 788 keV and is the first excited state of the nucleus. For ^{94}Mo the (^{3}He, d) study of Cates, Ball, and Newman[21] indicated that the 2066-keV level of ^{94}Mo is a positive-parity level with a spin of either 0 or 4. Our attempt to fit the inelastic scattering angular distribution as an $I^\pi = 4^+$ level gave a rather poor fit so we have assigned the level an $I^\pi = 0^+$.

The information deduced from the 0_0^+-2_1^+-$0_{1,2}^+$-$2_{1,2}^+$-$4_{1,2}^+$ coupling scheme is presented in Table V. In all cases the fits to the second 2^+ and first 4^+ states were improved by adding significant

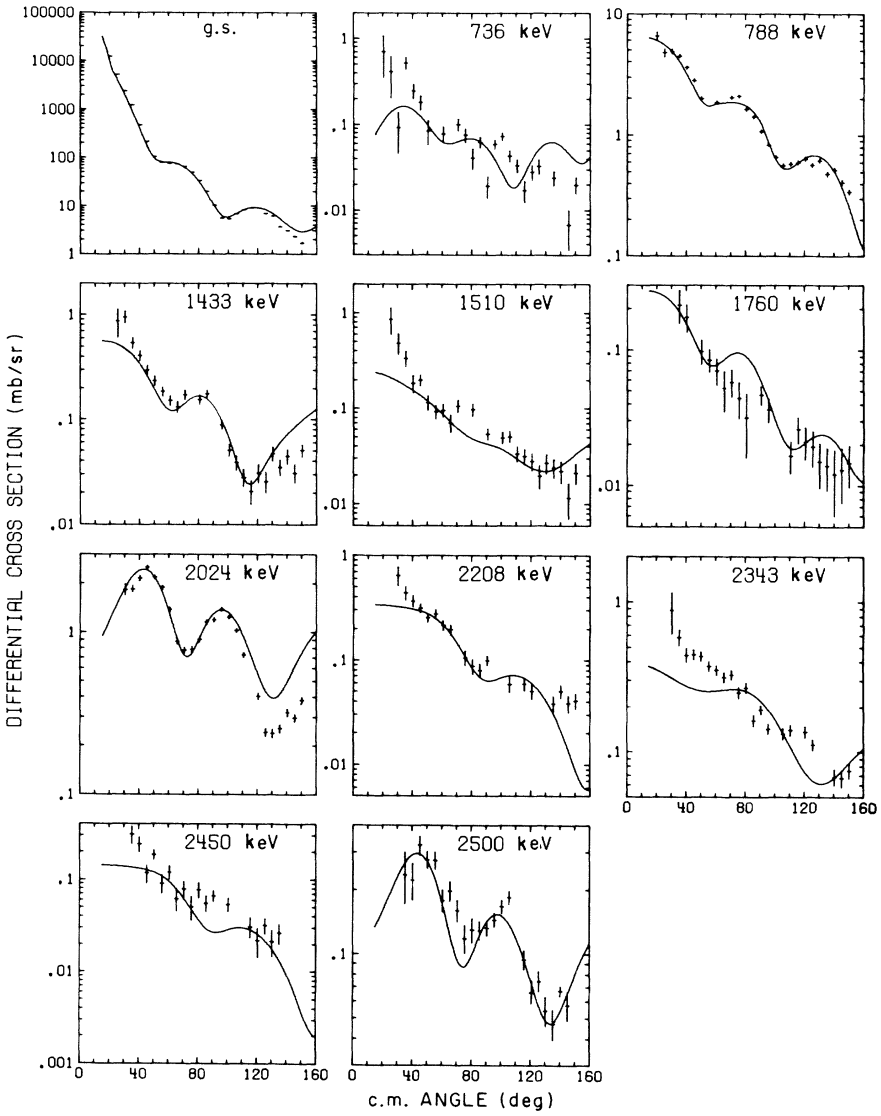

FIG. 5. Experimental results and theoretical fits for ^{98}Mo. The first excited state at 736 keV has $I^\pi = 0^+$.

amounts of single-phonon contributions. The β_{02} parameter is the coupling of the ground state to the one-quadrupole-phonon 2^+ state determined previously in the 0_0^+-2_1^+-3_1^- coupling scheme, and the parameters β_{20}, β_{22}, β_{24} are the strengths between the one- and two-phonon states. These coupling strengths arise from operators that are linear in α, where α is the coefficient of an expansion of the nuclear radius in spherical harmonics. In addition there are transitions from the ground state to the two-phonon states that are quadratic in α and denoted by the single-primed quantities β'_{00}, β'_{02}, β'_{04}. The double-primed quantities β''_{00}, β''_{02}, β''_{04} are linear in α and represent the coupling strengths between the ground state and the one-phonon admixtures. A measure of the one-phonon contribution can be taken from

$$\frac{(\beta''_{0I})^2}{\beta_{02}\times\beta_{2I}+(\beta''_{0I})^2}.$$

This quantity, expressed as a percentage, is entered in the last column of Table V. We see that with the exceptions of the 0^+ state in ^{96}Mo, ^{98}Mo, and ^{100}Mo and the 4^+ state in ^{100}Mo the single-step process allowed by the one-phonon admixture makes a larger contribution to the calculated cross section than does the two-step process that proceeds through the one-quadrupole-phonon state.

E. Results for 0_0^+-J_1^π Coupling Scheme Applied to ^{94}Mo, ^{96}Mo, ^{98}Mo, and ^{100}Mo

A number of generally weaker states were ana-

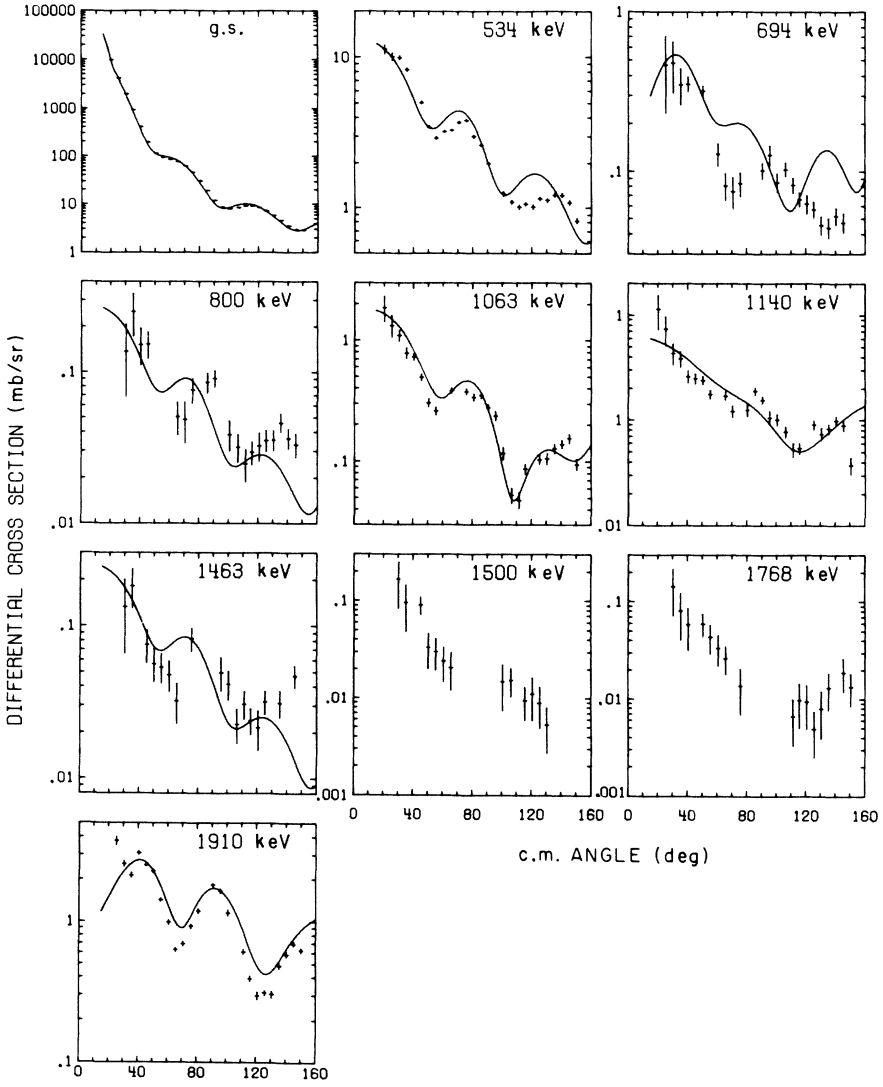

FIG. 6. Experimental angular distributions and theoretical fits for ^{100}Mo. No satisfactory fits were obtained for the levels at 1500 and 1768 keV.

TABLE V. Parameters of fits to state analyzed within the 0_0^+-2_1^+-$0_{1,2}^+$-$2_{1,2}^+$-$4_{1,2}^+$ coupling scheme.

Isotope	E_X (keV)	I^π	β_{02}	β_{0I} two phonon	β_{2I} two phonon	β''_{0I} one phonon	$\beta_{02}\times\beta_{2I}$	% of one-phonon contributions
^{94}Mo	2066	0^+		0.160	0.160	0.03	0.0256	58
	1864	2^+	0.160	0.160	0.160	−0.03	0.0256	58
	1573	4^+		0.160	0.160	0.08	0.0256	91
^{96}Mo	1147	0^+		0.175	0.175	0.0	0.0306	0
	1495	2^+	0.175	0.175	0.175	0.04	0.0306	63
	1624	4^+		0.150	0.150	0.04	0.0263	70
^{98}Mo	736	0^+		0.168	0.168	0.0	0.0282	0
	1433	2^+	0.168	0.168	0.168	0.04	0.0282	67
	1510	4^+		0.100	0.100	0.03	0.0168	76
^{100}Mo	694	0^+		0.226	0.226	0.0	0.0511	0
	1063	2^+	0.226	0.226	0.226	0.06	0.0511	58
	1140	4^+		0.170	0.170	0.02	0.0384	21

lyzed in terms of the simple 0_0^+-I_1^π coupling schemes, which correspond to the usual DWBA analysis. In no case did these states possess deformabilities that equalled the coupling strengths for the collective quadrupole or octupole vibrations. The information derived for these states is listed in Table VI. Most of the states listed in this table are positive-parity states. We do see a 5^- level in ^{94}Mo at 2580 keV, which corresponds to the 2527-keV level in ^{92}Mo and should be interpreted as $2p_{1/2}$ to $1g_{9/2}$ proton excitation. That we do not see the excitation of 5^- levels in the other isotopes of molybdenum is probably due to the increasing number of levels in the region of excitation studied and the limited resolution of the present experiment. In ^{98}Mo we see the only example of a second octupole state in the present experiment. It occurs at 2500 keV.

TABLE VI. Deformation parameters obtained from 0^+-I^π coupling schemes in ^{94}Mo, ^{96}Mo, ^{98}Mo, and ^{100}Mo.

Nucleus	E_X (keV)	I^π	β_{0I}
^{94}Mo	2421	2^+	0.04
	2580	5^-	0.07
	2830	4^+	0.06
	2930	2^+	0.04
	3090	2^+	0.05
^{96}Mo	1865	4^+	0.06
	2616	4^+	0.05
	2732	6^+	0.08
	2990	4^+	0.07
^{98}Mo	1760	2^+	0.03
	2208	2^+	0.06
	2343	6^+	0.11
	2450	4^+	0.04
	2500	3^-	0.06
^{100}Mo	800	2^+	0.03
	1463	2^+	0.03

We were unable to obtain satisfactory fits to three angular distributions. These were the 2810-keV level of ^{96}Mo and the 1500- and 1768-keV levels of ^{100}Mo.

F. Electromagnetic Transitions Rates Inferred from Deformabilities

The deformabilities that we have deduced in the inelastic proton scattering analysis may be used to infer electromagnetic transition rates. The expression based on a uniform charge distribution is

$$B(EL, 0 \rightarrow L) = [(\tfrac{3}{4}\pi) Z e R^L \beta_{0I}]^2 ,$$

$$R = R_{\mathrm{EM}} \times A^{1/3} = 1.2\, A^{1/3}\,\mathrm{fm} .$$

When the more realistic Fermi charge distribution is employed Owen and Satchler[34] have shown the necessity of a correction factor that is dependent on the multipole order. For the molybdenum isotopes we have followed Martens and Bernstein[18] and used 1.03, 1.13, 1.34, and 1.71 for $L = 2$, 3, 4, and 5. We also have the well-known relation[35]

$$\beta_{\mathrm{EM}} = \left(\frac{R_{\mathrm{CP}}}{R_{\mathrm{EM}}}\right)\beta_{\mathrm{CP}}$$

between the β deduced in the charged-particle experiment and that deduced in the purely electromagnetic interaction. If we express the transition rate in single-particle units given by

$$B(EL, 0 \rightarrow L)_{\mathrm{s.p.}} = \left[\frac{2L+1}{4\pi}\right]\left[\frac{3}{3+L}\right]^2 (R_{\mathrm{EM}})^{2L} e^2$$

and apply the corrections discussed above we obtain the prescription

$$G(L) = \frac{K(L)(1.25/1.20)^2(3+L)^2}{4\pi(2L+1)} Z^2 \beta_{0I}^2 .$$

IV. SUMMARY

We have measured the elastic and inelastic scattering of 15-MeV protons from ^{92,94,96,98,100}Mo. A total of 50 angular distributions were obtained and all but 3 of these were fitted with theoretical calculations made with a coupled-channel computer code. The experimental data were normalized by setting the forward angle elastic scattering equal to the optical-model predictions using parameters that we employed previously.[8] The good quality of the fits and the reasonable agreement with the quadrupole deformation parameters listed by Stelson and Grodzins[33] indicated that the normalization procedure was valid. For ^{92}Mo all the transitions were analyzed as single-step excitations. Some apparent discrepancies between the present experiment of Jaklevic, Lederer, and Hollander[19] were discussed and reconciled. By comparing our results with the α-particle scattering results of Martens and Bernstein[18] and showing that neither experiment excited the $I^\pi = 8^+$ levels we showed that the momentum of the incident projectile is not necessarily the limiting factor. One must also consider the limitations determined by the direct scattering mechanism. In the even-mass isotopes of molybdenum other than ^{92}Mo there were states that were analyzed in terms of the two-quadrupole-phonon triplet with admixtures of single-phonon states. A high degree of single-phonon admixture was found. A state with $I^\pi = 5^-$ and probably corresponding to the $2p_{1/2}$ to $1g_{9/2}$ proton excitation was seen in ^{92}Mo and ^{94}Mo. The deformabilities that were deduced in the present experiment were used to infer electromagnetic transition rates.

TABLE VII. Inferred electromagnetic transition rates expressed in single-particle units.

Isotope	E_x (keV)	I^π	β_{0I}	$G(L)$
^{92}Mo	1510	2^+	0.11	8.6
	2283	4^+	0.07	4.4
	2527	5^-	0.05	12.3
	2850	3^-	0.17	26.8
	3110	2^+	0.07	3.4
^{94}Mo	871	2^+	0.16	20.1
	2421	2^+	0.04	1.3
	2533	3^-	0.16	23.5
	2580	5^-	0.07	6.4
	2830	4^+	0.06	3.7
	2930	2^+	0.04	1.3
	3090	2^+	0.05	2.0
^{96}Mo	777	2^+	0.18	24.0
	1865	4^+	0.06	3.7
	2230	3^-	0.19	30.3
	2616	4^+	0.05	2.6
	2990	4^+	0.07	5.0
^{98}Mo	788	2^+	0.17	22.1
	1760	2^+	0.03	0.7
	2024	3^-	0.20	33.7
	2208	4^+	0.06	3.7
	2450	4^+	0.04	1.6
	2500	3^-	0.06	3.2
^{100}Mo	534	2^+	0.23	40.1
	1463	2^+	0.03	0.7
	1910	3^-	0.21	39.0

$G(L)$ is the value of $B(EL)$ expressed in single-particle units. The values for $G(L)$ are listed in Table VII.

*Work performed under the auspices of the U. S. Atomic Energy Commission.

[1]A. Bohr, Kgl. Danske Videnskab. Selskab, Mat.-Fys. Medd. 26, No. 14 (1952).
[2]K. Alder, A. Bohr, T. Huus, B. Mottleson, and A. Winther, Rev. Mod. Phys. 28, 432 (1956).
[3]A. Bohr and B. R. Mottelson, Kgl. Danske Videnskab. Selskab, Mat.-Fys. Medd. 27, No. 16 (1953).
[4]T. Tamura, Rev. Mod. Phys. 37, 679 (1965).
[5]T. Tamura, Oak Ridge National Laboratory Report No. ORNL-4152, 1967 (unpublished).
[6]H. F. Lutz, W. Bartolini, and T. H. Curtis, Phys. Rev. 178, 1911 (1969).
[7]H. F. Lutz, W. Bartolini, T. H. Curtis, and G. M. Klody, Phys. Rev. 187, 1479 (1969).
[8]T. H. Curtis, H. F. Lutz, and W. Bartolini, Phys. Rev. C 1, 1418 (1970).
[9]B. F. Bayman, A. S. Reiner, and R. K. Sheline, Phys. Rev. 115, 1627 (1959).
[10]I. Talmi and I. Unna, Nucl. Phys. 19, 225 (1960).
[11]K. H. Bhatt and J. B. Ball, Nucl. Phys. 63, 286 (1965).
[12]N. Auerbach and I. Talmi, Nucl. Phys. 64, 458 (1965).
[13]J. Vervier, Nucl. Phys. 75, 17 (1965).
[14]S. Cohen, R. D. Lawson, M. H. Macfarlane, and M. Soga, Phys. Letters 10, 195 (1964).
[15]J. B. Ball, J. B. McGrory, R. L. Auble, and K. H. Bhatt, Phys. Letters 29B, 182 (1969).
[16]W. A. Lanford, Phys. Letters 30B, 213 (1969).
[17]J. K. Dickens, E. Eichler, R. J. Silva, and I. R. Williams, Phys. Letters 21, 657 (1966).
[18]E. J. Martens and A. M. Bernstein, Nucl. Phys. A117, 241 (1968).
[19]J. M. Jaklevic, C. M. Lederer, and J. M. Hollander, Phys. Letters 29B, 179 (1969).
[20]K. P. Lieb, T. Hausmann, and J. J. Kent, Phys. Rev. 182, 1341 (1969).
[21]M. R. Cates, J. B. Ball, and E. Newman, Phys. Rev. 187, 1682 (1969).
[22]N. K. Aras, E. Eichler, and G. G. Chilosi, Nucl. Phys. A112, 609 (1968).
[23]J. Barrette, A. Boutard, and S. Munaro, Can. J. Phys. 47, 995 (1969).
[24]J. Eichler, Z. Physik, 219, 114 (1969).
[25]S. Antman, Y. Grunditz, A. Johansson, B. Nyman,

H. Pettersson, and B. Svan, Z. Physik 233, 275 (1970).
[26]W. J. Courtney and C. F. Moore, Phys. Letters 31B, 131 (1970).
[27]K. R. Evans and F. Ajzenberg-Selove, Phys. Rev. 165, 1327 (1968).
[28]K. Hubenthal, E. Monnand, and A. Moussa, Nucl.Phys. A128, 577 (1969).
[29]K. C. Chung, K. Swartz, A. Mittler, C. Robertson, T. D. Brandenberger, and M. T. McEllistrem, Bull. Am. Phys. Soc. 14, 1238 (1969).
[30]K. Swartz, J. D. Brandenberger, and M. T. McEllistrem, Bull. Am. Phys. Soc. 15, 807 (1970).
[31]G. R. Satchler, Nucl. Phys. A92, 273 (1967).
[32]P. Kossanyi-Demay and R. De Swiniarski, Nucl. Phys. A108, 577 (1968).
[33]P. H. Stelson and L. Grodzins, Nucl. Data A1, 21 (1965).
[34]L. W. Owen and G. R. Satchler, Nucl. Phys. 51, 155 (1964).
[35]J. S. Blair, in *Lectures in Theoretical Physics*, edited by P. D. Kunz and W. E. Brittin (University of Colorado Press, Boulder, Colorado, 1966), Vol. VIII, p. 396.

PHYSICAL REVIEW C VOLUME 4, NUMBER 3 SEPTEMBER 1971

Neutron Emission from Prompt Fragments in the Fission of Excited Nuclei

Ratna Sarkar
Saha Institute of Nuclear Physics, Calcutta-9, India

and

Aparesh Chatterjee
Calcutta University, Calcutta, India, and Saha Institute of Nuclear Physics, Calcutta-9, India

(Received 28 September 1970; revised manuscript received 19 May 1971)

Our improved approach combining the renormalized Fermi-gas model (RGM) with the use of an average collective potential energy surface (PES) has been used to estimate the energy release in prompt fission phenomena from fission of excited nuclei. The role of excess excitation ΔU_I on top of the fission barrier, under several assumed constraints, is discussed. The partition of ΔU_I into the conjugate prompt fragments has been calculated from a simple RGM saturation condition. The practical limits of ΔU_I have been discussed from the viewpoint of the statistical model of nuclear reactions. The number of evaporated neutrons from the prompt fragments ν_F has been estimated from LeCouteur and Lang's approximation using Wing and Varley's neutron binding-energy tables. Fairly satisfactory agreement for the number ν_F has been obtained with the experimental work on fission of ^{230}Th by 25.7- and 29.5-MeV ^{4}He ions and of ^{226}Ra by 13.0-MeV protons. A linear relationship of the average number of prompt neutrons $\bar{\nu}$ with ΔU_I is predicted from our model.

1. INTRODUCTION

Our preliminary work[1,2] on the fission energy kinetics at the saddle-scission point combined two interdependent models of nuclear structure – the renormalized Fermi-gas model[1-3] (RGM) and Mosel and Greiner's formulation[4] in terms of an average collective potential energy surface (PES). A concept similar to our RGM was applied by Ignatyuk[5] to fission at about the same time (1966–69).

The RGM treats the static nuclear structural energies in a unfilled shell system at a ground-state deformation β as an energy correction $\partial\epsilon$ on the free-gas Fermi surface ϵ_0 in a self-consistent way without using any free parameters. The RGM correction $\partial\epsilon$ contains the effects of long- and short-range parts of the nuclear interactions:

$$\epsilon = \epsilon_0 + \partial\epsilon = \epsilon_0 + f - \Delta^2/G - \delta\,, \qquad (1)$$

where f is the single-particle combinatorial energy correction[6-8] (Rosenzweig term), and Δ^2/G and δ are the pairing interaction and ground-state deformation energy corrections, respectively, evaluated from the Belyaev model.[9] The even-even system is further bound by an amount of energy of the order of the pairing gap Δ.

The RGM correction $\partial\epsilon$ determines the energy region in which the sharp Fermi level is diffused as a result of nuclear interactions. From the viewpoint of gas models, $\partial\epsilon$ may also be interpreted as a measure of the entropy of a nuclear Fermi gas at a nonzero ground-state temperature.

The average-PES concept treats the shape deformation-dependent parts of the nuclear energy expanded in power series of the different deformation degrees. The total PES energy of a system may be written as a sum of BCS plus Coulomb energies of a nucleus A consisting of Z protons and